Chirped solitons as attractors for short light pulses

Marcus Neuer, Karl H. Spatschek,* and Zhonghao Li†
Institut für Theoretische Physik, Heinrich-Heine-Universität Düsseldorf, D-40225 Düsseldorf, Germany
(Received 28 May 2004; published 15 November 2004)

Nonlinear chirped pulse solutions are shown to exist as stable attractors for short light pulses in driven and damped systems. The attractors are determined for systems of different complexity, from simple gain and damping modelings up to the inclusion of higher-order dispersion, Raman processes, and delayed nonlinear responses. The chirped attractors, their stability, as well as the attractor basins can be determined analytically. The analytical predictions are in excellent agreement with numerical simulations.

DOI: 10.1103/PhysRevE.70.056605 PACS number(s): 42.65.Tg, 05.45.Yv, 42.79.Sz, 42.81.Dp

I. INTRODUCTION

Localized structures are important objects of nonlinear dynamics in driven and dissipative systems far from equilibrium. The cubic, complex Ginzburg-Landau equation (CGLE) is one of the most-studied nonlinear models in such systems. It allows us to understand a vast variety of phenomena, e.g., self-trapping of light, second-order phase transitions, superconductivity, superfluidity, Bose-Einstein condensation, liquid crystals, strings in field theory, particle acceleration in relativistic plasmas, and so on (see, e.g., [1] and references therein). In some areas, the CGLE appears as a generalized or higher-order nonlinear Schrödinger equation (HNLSE). The integrable (cubic) nonlinear Schrödinger equation (NLSE) is the weakly nonlinear and weakly dispersive paradigm for envelope radiation pulses. The nonlinear short-pulse propagation requires further generalizations of the NLSE leading to a one-dimensional CGLE or HNLSE [2–6] by taking into account, e.g., dispersive-type higher-order terms [such as third-order dispersion (TOD), nonlinear dispersion, and self-frequency shift (SFS) arising from stimulated Raman scattering].

The models were further extended, particularly for intensive and short light pulses whose widths are shorter than 100 fs. Then, in addition to the dispersive-type effects mentioned above, also the driven and dissipative-type effects, such as spectral limitation due to gain bandwidth-limited amplification and/or spectral filtering, nonlinear gain and/or absorption with fast and/or slow delayed nonlinear response, etc., may play important roles. With quite general arguments, Gagnon and Bélanger [7] have derived a generalized integro-differential equation to describe the propagation of a nonlinear radiation pulse. They analyzed some of its properties by employing adiabatic perturbation methods [7].

Many authors [8–18] have analyzed HNLSEs from different points of view (e.g., Painlevé analysis, Hirota direct method, inverse scattering transform, Darboux-Bäcklund transform, etc.). They obtained solitonlike solutions under the balance between group velocity dispersion (GVD), self-phase modulation (SPM), TOD, and self-steepening effects, respectively. The research results have shown the complexity, multiplicity, and richness of phenomena in driven and damped nonlinear short-pulse physics [19–26].

The unique stability of short-pulse solitons, enabled by the capability of balancing the dispersion and nonlinearity, is a very important phenomenon compared to linear (nonsoliton) systems. A decisive point is the possibility of compensating losses by amplification. In this paper, we investigate different practical forms for gain and damping processes. The unique results of the various investigations are that attractors in forms of solitonlike pulses do exist. An important characteristic of the attractors is the chirp. Knowing the analytical forms of attractor solutions, we are able to predict the dynamics of the pulse parameters, such as amplitude, width, and chirp. Motivated by numerical simulations, reduced models of the driven and damped HNLSE are proposed by means of Lagrangian perturbation theory. The analytically determined solutions of these problems are shown to be attractors for a variety of initial values. Stability analysis of the attractors leads to characterizations of the basins of attractions in the cases of balanced gain and damping, and shows new phenomena such as short-pulse generation when amplification and damping are not balanced.

In this paper, we present the exact chirped solitonlike solution for a fs laser pulse, including not only dispersive-type effects but also the driven and dissipative-type contributions. It will have its application in ultrashort optical pulse propagation in nonconservative systems. As a very important generalization compared to recent findings [27], we are able to take into account the delayed nonlinear response which was not considered previously. We will discuss the dependence of the pulse widths on the parameters of the system as well as the stability with respect to the finite amplitude perturbations.

The paper is organized as follows. In the next section, we present the general model. That model is analyzed in full generality in Sec. III. In Appendix A, we discuss a simplified version which has been often used in the literature. At the simplified model, we explain what is meant by the core and tail stability problems, respectively. There, also the main tools, such as numerical simulation, collective coordinates, and perturbation theory, are demonstrated for a case which is easier to look through. Nevertheless, new results are already

*Electronic address: spatschek@thphy.uni-duesseldorf.de
†Present address: Department of Electronics and Information Technology, Shanxi University, Taiyuan, Shanxi 030006, People's Republic of China.

presented there, and discrepancies in the literature are clarified. Solitary solutions in the general case are demonstrated in Sec. III. Analytical predictions are compared with numerical simulations. The Lagrangian method for collective coordinates turns out to be a very effective tool for quite precise predictions. The main conclusion of this section will be that solitary attractors with stable tails do exist. The paper is concluded by a short summary (Sec. IV).

II. GENERAL MODEL

A quite general model for the propagation of femtosecond (e.g., 100 fs) pulses is [3,7]

$$iq_z + \frac{1}{2}q_{tt} + |q|^2 q = i\delta q - \gamma q_t + i\beta q_{tt} + i\chi|q|^2 q + i\lambda q_{ttt} + i\mu(|q|^2 q)_t + i\nu q(|q|^2)_t + i\kappa q\int_{-\infty}^{t}|q|^2 dt + i\sigma q_t\int_{-\infty}^{t}|q|^2 dt \equiv iR[q,q^*]. \quad (1)$$

Here, $q(z,t)$ is the complex envelope of the electric field, z is the normalized propagation distance, and t is the retarded time. The model parameters δ, γ, β, and χ are real constants; λ, μ, ν, κ, and σ can be complex. Anomalous dispersion is assumed. Furthermore, $\delta>0$ (<0) is the linear excess gain (loss) at the carrier frequency ω_0; γ and the imaginary part λ_i of λ result from the difference between the pulse carrier frequency ω_0 and the gain-center frequency ω_a (and are proportional to $\delta\omega=\omega_a-\omega_0$), β describes the effect of spectral limitation due to gain bandwidth-limited amplification and/or spectral filtering (which are inversely proportional to gain and/or spectral filtering bandwidth, respectively); χ accounts for nonlinear gain and/or other absorption processes. The real part λ_r of λ represents the net TOD from material. The real part μ_r of μ is the nonlinear dispersion term; it is responsible for self-steepening at the pulse edge. The imaginary part μ_i of μ describes the combined effect of nonlinear gain and/or absorption processes; ν is the nonlinear gradient term which results from the time-retarded induced Raman process; its imaginary part ν_i is usually responsible for the soliton self-frequency shift [2]; κ and σ result from the possible slow delayed response of nonlinear gain and/or absorption effects. We would like to emphasize that mathematically the delay terms, being proportional to κ and σ, change the type of the problem to an integro-differential equation.

III. SOLITARY ATTRACTORS

In this section, we shall show that realistic chirped soliton attractors with stable tails result from the general model (1) provided relevant physical effects are included. This is very important since, as we show in Appendix A, (extremely) simplified models which have been extensively used in the literature do not lead to soliton attractors with stable tails. Thus, the additional effects discussed here are very important for practical applications.

A. Analytical predictions

From the mathematical point of view, Eq. (1) is a highly nontrivial, nonconservative partial differential equation. In general, its solution is not known. Nevertheless, it is interesting to note that for the general case, the form of the stationary soliton solutions, which act as attractors, can be determined analytically. In the following, we first describe the recipe to find analytical soliton expressions.

1. Motivation of the ansatz

We start with the analysis of Eq. (1) by separating $q(z,t)$ into a real amplitude envelope function $A(z,t)$ and a phase shift $\phi(z,t)=\Omega t-Kz+\varphi(z,t)$ according to $q(z,t)=A(z,t)\exp[i\phi(z,t)]$. Here $\varphi(z,t)$ denotes a possible nonlinear phase shift. Substituting the ansatz into Eq. (1), and assuming both the envelope function $A(z,t)$ and the nonlinear phase $\varphi(z,t)$ to be even functions, we can decouple Eq. (1) into two equations, namely,

$$(i\gamma_0+\gamma_6C_1)A + i\gamma_2(A_{2\tau}+i\varphi_{2\tau}A+i2\varphi_\tau A_\tau-\varphi_\tau^2 A)+i\gamma_n A^3 - \sigma B(A_\tau-i\varphi_\tau A)=0, \quad (2)$$

$$(\gamma_1-\rho)(A_\tau+i\varphi_\tau A)-\lambda[A_{3\tau}+i3\varphi_\tau A_{2\tau}+3(i\varphi_{2\tau}-\varphi_\tau^2)A_\tau + (i\varphi_{3\tau}-3\varphi_\tau\varphi_{2\tau}-i\varphi_\tau^3)A]-\mu A^2(3A_\tau+i\varphi_\tau A)-\nu 2A_\tau A^2 + \gamma_6 AB-\sigma C_1(A_\tau-i\varphi_\tau A)=0. \quad (3)$$

Here $\tau=t-\rho z$ is the retarded time, $\int_{-\infty}^{t}A^2dt=\int_{-\infty}^{\tau}A^2d\tau=B(\tau)+C_1$, with $C_1=B(\tau)|_{\tau\to\infty}$, and the parameters γ_i are defined as $\gamma_0=-K+\Omega^2/2+\lambda_r\Omega^3+i(\delta-\gamma\Omega-\beta\Omega^2+\lambda_i\Omega^3)$, $\gamma_1=-i\gamma+2(1/2-i\beta)\Omega-3\lambda\Omega$, $\gamma_2=-(1/2-i\beta)\Omega-3\lambda\Omega$, $\gamma_n=-(1-i\chi)-\mu\Omega$, and $\gamma_6=-\kappa-i\sigma\Omega$. When setting

$$A_\tau/A = B/C_2 = \varphi_\tau/C_3, \quad (4)$$

where the coefficients C_2 and C_3 are constants (to be determined later), Eqs. (2) and (3) are compatible under the conditions

$$[i\gamma_2(1+iC_3)-\sigma C_2]\left(\gamma_1-\rho+\frac{\gamma_6C_2}{1+iC_3}-\sigma C_1\right) = -\lambda(1+iC_3)(i\gamma_0+\gamma_6C_1), \quad (5)$$

and

$$[i\gamma_2(2+iC_3)-\sigma C_2]\left(\mu+\frac{2\nu}{3+iC_3}\right)=i\gamma_n\lambda(2+iC_3). \quad (6)$$

It is easy to prove that subject to zero-boundary conditions Eq. (3) has the following localized solution:

$$A(\tau)=A_0\,\mathrm{sech}(\eta\tau), \quad (7)$$

for

$$(i\gamma_0+\gamma_6C_1)+[i\gamma_2(1+iC_3)-\sigma C_2](1+iC_3)\eta^2=0, \quad (8)$$

$$i\gamma_nA_0^2-[i\gamma_2(2+iC_3)-\sigma C_2](1+iC_3)\eta^2=0. \quad (9)$$

The compatibility conditions (5) and (6) can now be written in more convenient forms,

$$\left(\gamma_1 - \rho + \frac{\gamma_6 C_2}{1+iC_3} - \sigma C_1\right) - \lambda(1+iC_3)^2\eta^2 = 0, \quad (10)$$

$$\left(\mu + \frac{2\nu}{3+iC_3}\right)A_0^2 - \lambda(1+iC_3)(2+iC_3)\eta^2 = 0. \quad (11)$$

Substituting the solution (7) into $\int_{-\infty}^{t} A^2 dt = B(\tau) + C_1$ and making use of Eq. (4), we can determine $C_1 = A_0^2/\eta$, $C_2 = AB/A_\tau = -A_0^2/\eta^2$, and $\varphi = -C_3 \ln[\cosh(\eta\tau)]$. The parameter C_3 will be determined by Eqs. (8)–(11). Obviously, the parameter C_3 denotes the chirp strength.

Making use of all these findings, we can present the solution of Eq. (1) as

$$q(z,t) = A_0\{\mathrm{sech}[\eta(t-\rho z)]\}^{1+iC_3}\exp\{i[\Omega(t-\rho z) - Kz]\}. \quad (12)$$

The form (12) has been extensively used as an ansatz in many dynamical equations, e.g., for NLSE, HNLSE, and the CGLE, also including the nonlinear term of slow response time [27]. Directly substituting the solution (12) into Eq. (1) and requiring the coefficients of independent terms of hyperbolic secant functions to vanish separately, relations (8)–(11) will appear. It implies that, similar to the case of NLSE, physical effects in each equation balance each other to form the solitonlike solution (12).

2. Evaluation of the parameters

In the following, we concentrate on the general properties of the solitonlike solution. We first evaluate the pulse parameters in explicit forms.

Equations (8)–(11) are four complex equations. They can determine eight real parameters. From the real and imaginary parts of Eq. (11) one can find the algebraic equation for the chirp parameter C_3,

$$m_1 C_3^4 + (2m_3 - 3m_4)C_3^3 + (7m_1 - 12m_2)C_3^2 - (22m_3 + 27m_4)C_3 + 6(2m_2 - 3m_1) = 0. \quad (13)$$

Here we have set $m_1 = (\lambda_i\mu_r - \lambda_r\mu_i)$, $m_2 = (\lambda_r\nu_i - \lambda_i\nu_r)$, $m_3 = (\lambda_r\nu_r + \lambda_i\nu_i)$, and $m_4 = (\lambda_r\mu_r + \lambda_i\mu_i)$.

Equation (13) indicates that the chirp is strongly dependent on the higher-order dispersive, nonresonance, self-steepening, and self-frequency shift effects. Only if the very specific condition $3(\lambda_i\mu_r - \lambda_r\mu_i) = 2(\lambda_r\nu_i - \lambda_i\nu_r)$ is satisfied is a proper balance available, and no chirp occurs. Thus, a solitary-wave solution without chirp can exist in dispersive systems (such as the NLSE and HNLSE) only under quite restrictive conditions.

Combining the imaginary part of Eq. (9) and the real part of Eq. (11), one can determine the frequency shift

$$\Omega = \frac{(1 + \sigma_r C_3 + \sigma_i)n^2 - 3C_3\beta - (2 - C_3^2)/2}{3\lambda_r(2 - C_3^2) - 9\lambda_i C_3 - \mu_r n^2}, \quad (14)$$

where we have defined $n^2 \equiv A_0^2/\eta^2 = [6(1-C_3^2)\lambda_r - C_3(11 - C_3^2)\lambda_i]/(3\mu_r + 2\nu_r - C_3\mu_i)$.

The imaginary part of Eq. (10) and the real part of Eq. (11) lead to the parameter being inversely proportional to the pulse width η,

$$\eta = -\sigma_i n^2/2m_5 \pm [\gamma_{1i} - m_6 + \sigma_i^2 n^4/4m_5^2]^{1/2}, \quad (15)$$

where $m_5 = 2C_3\lambda_r + \lambda_i(1 - C_3^2)$, $m_6 = (\gamma_{6i} - \gamma_{6r}C_3 n^2)/(1 + C_3^2)$. The pulse amplitude A_0 can be derived from the imaginary part of Eq. (11),

$$A_0 = \eta\sqrt{\frac{6(1-C_3^2)\lambda_i + C_3(11 - C_3^2)\lambda_r}{3\mu_i + 2\nu_i + C_3\mu_r}}. \quad (16)$$

The amplitude shift parameter ρ and the phase shift parameter K are determined by the imaginary part of Eq. (8) and the real part of Eq. (10), respectively. Finally, the real parts of Eq. (8) and Eq. (9) will give the constraints on the model parameters so that the stationary soliton solution (12) can exist.

Summarizing, narrow, chirped solitonlike pulse forms of Eq. (1) can be calculated systematically in the form (12). The parameters follow from algebraic equations.

3. Specific dependences

Generally, the properties of the solitonlike pulses are complicated and difficult to investigate analytically because of the complex dependences on the model parameters. Here we present only one example to show the dependence of the pulse widths on the parameters chirp γ, frequency shift Ω, TOD λ_r, gain-band-limitation and/or spectral filter, SFS, and slow delayed response to nonlinear gain and/or absorption χ numerically. We have found that for the coefficients $\delta = -3.25\times10^{-3}$, $\gamma = 1.019\times10^{-2}$, $\beta = 0.853$, $\chi = 0.224$, $\lambda_r = -5.367\times10^{-2}$, $\lambda_i = 1.263\times10^{-3}$, $\mu_r = -2\times10^{-2}$, $\mu_i = -10^{-2}$, $\nu_r = -2\times10^{-2}$, $\nu_i = -5\times10^{-2}$, $\kappa_r = 10^{-2}$, $\kappa_i = 7\times10^{-3}$, $\sigma_r = 4\times10^{-3}$, and $\sigma_i = -3\times10^{-3}$, the solitonlike solution (12) has the parameters $A_0 = 0.58$, $\eta = 0.38$, $\Omega = 2\times10^{-3}$, $C_3 = 0.586$, $\rho = 2.823\times10^{-2}$, and $K = -0.198$. As shown in Fig. 1(a), narrower pulses will occur for the positive chirp than for the negative chirp. Figures 1(b) and 1(c) indicate that the larger frequency shift and the smaller absolute TOD will lead to the narrower pulse widths. The former has been observed in some laser systems and fiber amplifiers (see, e.g., [28–30]), and the latter is consistent with the well-known experimental results from ultrashort-pulse lasers. From Figs. 1(d)–1(f), we can recognize that larger spectral filter, larger SFS effects, and stronger slow saturable absorption will produce narrower pulses.

By numerical simulations of Eq. (1), we have proven the stability of that solution. Note that for this solution, together with the core, also the tails are stable.

B. Lagrangian methods

The analytical treatments suggest that the attractor of Eq. (1) can be written in the explicit analytical form

$$q(z,t) = A\{\mathrm{sech}[\eta(t-T)]\}\exp(iC\log\{\mathrm{sech}[\eta(t-T)]\}) \times \exp\{i[\Omega(t-T)] + iK\}. \quad (17)$$

As has been shown, in some ranges, the six parameters A, η, C, $T(z)$, $K(z)$, and Ω can be calculated exactly from algebraic relations by methods similar to [22].

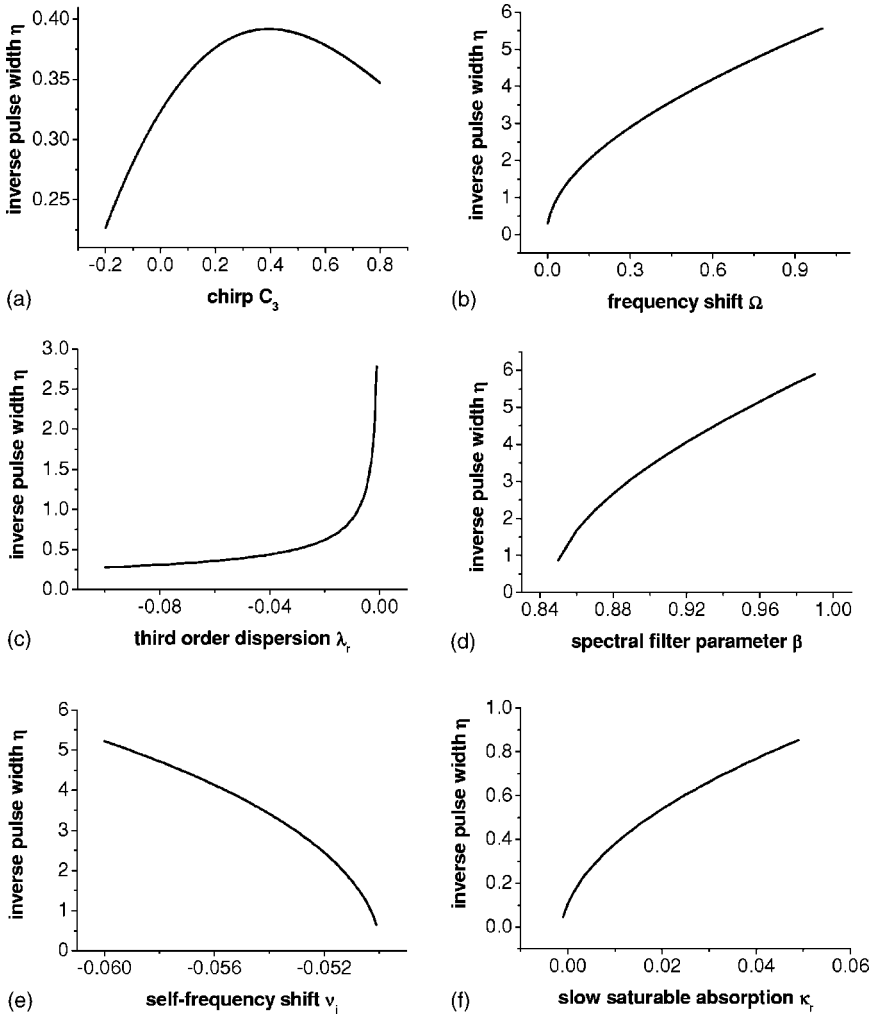

FIG. 1. Asymptotic numerical solutions of Eq. (1) for different parameter values, but without delayed responses. The inset shows the amplitude predictions by the Lagrangian momentum method. We find attractors with stable tails.

As we will show next, the Lagrange methods can be used to predict the analytical values in accordance with numerical simulations.

The Lagrangian method is extensively demonstrated in the Appendix A. Thus, here we immediately go to the explicit results. Using Eq. (17), the time-integrated Lagrangian density reads

$$L_0 \equiv L_0(A,A',\eta,\eta',C,C',T,T',K,K',\Omega,\Omega') = \frac{2A^4}{3\eta} - \frac{1}{3}\eta^2 A(1+C)^2 - \frac{A^2\Omega^2}{\eta} - \frac{2A^2K'}{\eta} + \frac{2A^2\Omega T'}{\eta} + \frac{2A^2C'}{\eta} - \frac{\log(4)A^2C'}{\eta} + \frac{A^2C\eta'}{\eta^2}. \quad (18)$$

This form is a generalization of the Lagrangian shown in Appendix A. Here we have added a time shift $T=T(z)$.

1. Collective coordinates

Within this formulation, the parameters A,η,C,T,K, and Ω are the coordinates $[\hat{=}x_i, i=1,2,\ldots,6]$, and the derivatives $[\hat{=}x_i', i=1,2,\ldots,6]$ correspond to velocities, being designated as primed quantities, i.e., $A' \equiv dA/dz$ and so on. The fixed points of the corresponding six modified Euler-Lagrange equations

$$\frac{d}{dz}\left(\frac{\partial L_0}{\partial x_i'}\right) - \frac{\partial L_0}{\partial x_i} = i\varepsilon \int_{-\infty}^{+\infty} dt\left(R^*\frac{\partial q}{\partial x_i} - R\frac{\partial q^*}{\partial x_i}\right) \quad (19)$$

for $i=1,2,\ldots,6$ determine the chirped soliton dynamics in the representation (17). In Appendix B, we present the details of the Euler-Lagrange equations.

2. Comparison with numerical solutions

Next, we have compared the numerical solutions of Eq. (1) with predictions by Eqs. (B2)–(B6). The stationary solutions (fixed points) agree exactly. In general, we can say that the Lagrangian perturbation theory predicts the dynamics very well.

Without delayed response ($\kappa=\sigma=0$), in Fig. 2 a soliton solution is shown for the parameters $\delta=-0.001\,51$, $\gamma=0.062\,93$, $\beta=0.509\,67$, $\chi=0.191\,58$, $\lambda_r=-0.032\,04$, $\lambda_i=0.007\,72$, $\mu_r=-0.041\,37$, $\nu_i=-0.0256$, and $\mu_i=\nu_r=0$. The soliton parameters are $A=0.815\,85$, $\eta=0.653\,33$, $C=0.4182$, and $\Omega=-0.053\,115$. That completely stable solution is marked as initial since we use it in the next step as an initial pulse (which evolves in z) in Eq. (1) with $\lambda_r=-0.042$ and $\lambda_r=-0.02$, respectively. The other parameters are unchanged. The numerically determined asymptotic and stable solutions are also shown in Fig. 2 (with the characterization numeri-

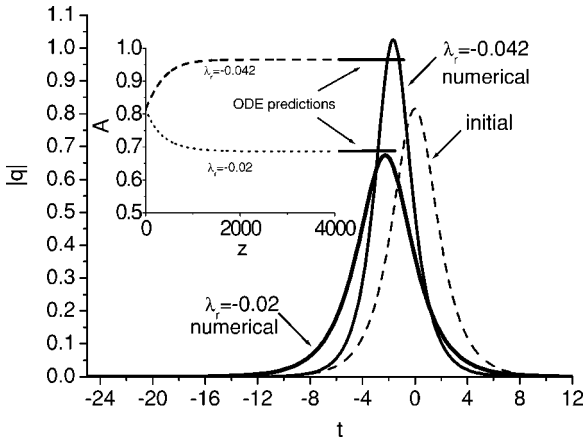

FIG. 2. Asymptotic numerical solutions of Eq. (1) for different parameter values, but without delayed responses. The inset shows the amplitude predictions by the Lagrangian momentum method. We find attractors with stable tails.

cal). In parallel to the numerical simulations, we have solved the Euler-Lagrange equations (B2)–(B6). The z dependence of the amplitude A is shown as the inset in Fig. 2 for the two λ_r values, respectively. The predicted amplitudes (bars) agree quite well with the numerics.

Next, we discuss the influence of a delayed response and show that stable chirped attractors exist also in that situation. In Fig. 3, we again start with an exact solution for $\kappa=\sigma=0$ by using the same parameter values as in Fig. 2. Then we put this form as the initial pulse into Eq. (1), after changing $\kappa_r=0$ into $\kappa_r\neq 0$, leaving the other parameters unchanged. For demonstration, we set $\kappa_r=0.001$. New attractors appear for $\kappa_r\neq 0$ which have quite different forms, depending on the chosen values of κ_r. However, they belong to the class of exact solutions (17) mentioned above. The (first-order) Lagrangian prediction [i.e., Eq. (17) with parameter values determined from Eqs. (B2)–(B6)] is also shown. Again, the agreement is quite good.

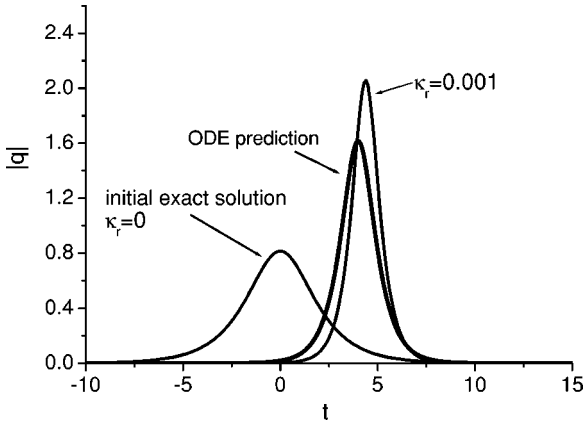

FIG. 3. Asymptotic numerical solution of Eq. (1) in the case of a delayed response. The prediction by the Lagrangian momentum method is shown for comparison. We find attractors (at $z=4000$) with stable tails.

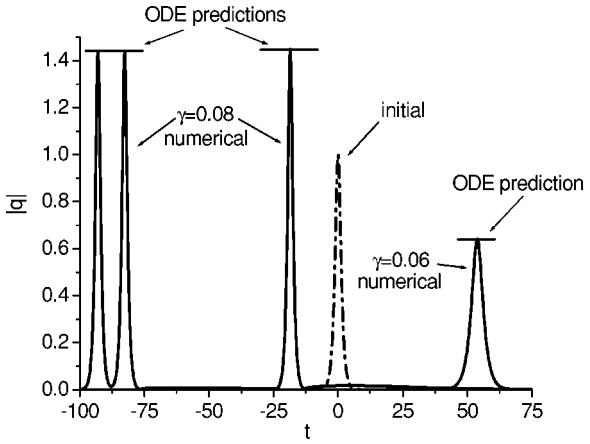

FIG. 4. Numerical solutions of Eq. (1). An unstable situation ($\gamma=0.08$) is compared with a stable case ($\gamma=0.06$). In the unstable situation, pulses are generated, but in all cases the Lagrangian momentum method predicts the right core parameters (the predicted amplitudes are shown as bars).

C. Stability of the tails

So far we have considered attractors with stable tails. However, for strong gains, the system cannot adjust itself in stable forms. Then the tails become unstable, and new solitons are generated. Figure 4 shows the evolution of an initial pulse with $A=\eta=1, C=T=\Omega=K=0$ when evolved according to Eq. (1) (with the same parameters as in Fig. 2, except for $\gamma=0.08$ and $\gamma=0.06$, respectively). We have varied the driving through the $-\gamma q_t$ term on the right-hand side of Eq. (1). In the unstable case $\gamma=0.08$, new solitons of the same form are generated. It is noteworthy that in all cases the individual pulses have the form (17) with parameters following from the fixed points of Eqs. (B2)–(B6). When $\gamma=0.06$, i.e., in the stable situation, again a single stable soliton appears as an attractor. For much smaller values of γ, dissipation is dominant, and the initial pulse damps out.

The adjustment between (linear and nonlinear) driving and damping processes is a complicated process which, in general, is not easy to handle analytically. We can consider tail perturbations of the form $\exp(ikz-i\omega t)$ and determine the imaginary part of k. When the first three terms on the right-hand side of Eq. (1) dominate the energy input and damping of the tails, we obtain

$$-\mathrm{Im}\ k \approx \delta-\beta\omega^2+\gamma\omega. \tag{20}$$

Then, stable tails can be expected for

$$\delta+\frac{\gamma^2}{4\beta}<0. \tag{21}$$

This limit agrees with the numerical findings for long tails; the presence of the core changes it a little bit. In addition, when the other (nonlinear) gain and damping terms become important, the tail stability criterion becomes modified.

IV. SUMMARY AND CONCLUSIONS

Summarizing, we have developed and applied methods for identifying stable chirped attractors in quite general

short-pulse models. In Appendix A, we investigated a simple model which has been used in the literature many times. Our analysis shows that no stable (core and tails) attractor exists for that simple case. More complex models, including various other important physical effects, were discussed in the main part of the paper. Now stable attractors could be identified.

The techniques developed here allow the fast finding of stable attractors. One reason is that the attractors can be presented in analytical form. In addition, the excellent applicability of the results of the Lagrangian perturbation theory allows us to identify optimal conditions for narrow pulse propagation under complex physical conditions.

ACKNOWLEDGMENTS

This work had been performed within the SFB/Transregio TR 18. Z.L. wishes to thank the Deutsche Forschungsgemeinschaft for support through the Graduiertenkolleg of the Heinrich-Heine-Universität Düsseldorf.

APPENDIX A: SOLITARY SOLUTIONS FOR A SIMPLIFIED CASE

This appendix is devoted to the frequently used simplified model for $\gamma=\chi=\lambda=\mu=\nu=\kappa=\sigma=0$. Then we have the relatively simple model

$$iq_z + \frac{1}{2}q_{tt} + |q|^2 q = i\delta q + i\beta q_{tt}, \tag{A1}$$

which contains gain δ and damping β. In an earlier approach, Hasegawa and Kodama [2] derived a reduced model for Eq. (A1) by applying adiabatic perturbation theory on the standard soliton solution. It led to a predicted attractor without chirp. Pereira and Stenflo [31], on the other hand, found an exact solution of Eq. (A1),

$$q(z,t) = A[\mathrm{sech}(Bt)]^{1+iC}\exp(iDz), \tag{A2}$$

which contains the real parameters amplitude A, width B, chirp C, and phase D. Inserting Eq. (A2) into Eq. (A1), one gets relations between the parameters and their dependences of δ and β, namely

$$A^2 = B^2\left(1 + 3\beta C - \tfrac{1}{2}C^2\right), \tag{A3}$$

$$B^2 = \frac{\delta}{\beta - \frac{1}{2}C}, \tag{A4}$$

$$C = -\frac{3}{4\beta} \pm \sqrt{\left(\frac{3}{4\beta}\right)^2 + 2}, \tag{A5}$$

$$D = A^2 - \tfrac{1}{2}B^2 - \beta B^2 C. \tag{A6}$$

As the exact solution has a nonvanishing chirp, it is surprising that the attractor presented by Hasegawa and Kodama has no chirp.

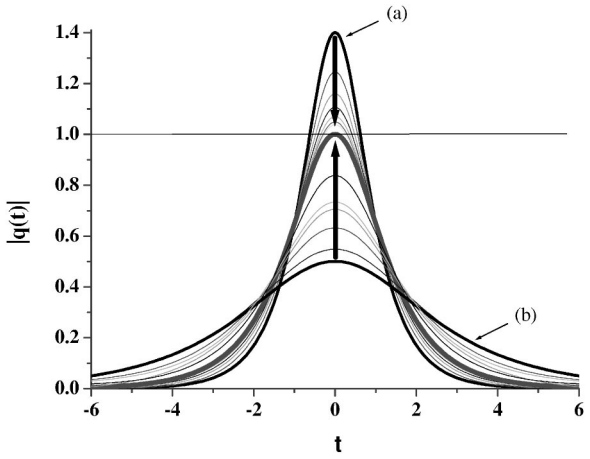

FIG. 5. Numerical simulation of Eq. (A1) for two initial distributions (a) and (b), respectively. The parameter values are $\delta=0.01$ and $\beta=0.03$. Shown is the approach to the attractor (A2) with increasing z values.

1. Core stability

a. Numerics on a finite time domain

We first consider the problem of solitary solutions in the simplified model and solve Eq. (A1) numerically. The numerics suggests, for different initial pulses, that the final solution (attractor) is given by Eq. (A2). Figure 5 shows the shape variation of two initial pulses (a) and (b), respectively, which approach the exact solution (normalized amplitude 1) while traveling along the z axis. The results were obtained by a numerical simulation of Eq. (A1) using an operator-splitting algorithm on a finite time domain. When the extension of the time domain is not too large, that type of numerics can only conclude on the core stability of the proposed solution. We shall come back to the tail stability later.

The analytical solution only exists for $\delta/\beta > 0$. Numerics further shows that for stable cores $\delta > 0$ is required. This result can be understood by the arguments presented in the following subsections.

b. Collective coordinates

We next present analytical arguments that the exact solution (A2) can be considered as the stable attractor core. First, we use a Lagrangian momentum method which reduces the rather complex partial differential equation to a set of ordinary differential equations (ODEs). For the derivation of the ODE model, we use a Lagrangian perturbation theory [2] for adiabatic perturbations. The idea is the following. We first write the basic equation in the form

$$iq_z + \frac{1}{2}q_{tt} + |q|^2 q = i\varepsilon R[q,q^*]. \tag{A7}$$

The right-hand side contains perturbation terms summarized by R. The unperturbed cubic nonlinear Schrödinger equation ($R \equiv 0$) has the Lagrangian density

$$\mathcal{L}_0[q,q^*] = \frac{i}{2}(q^* q_z - q_z^* q) + \frac{1}{2}(|q|^4 - |q_t|^2). \tag{A8}$$

The basic equation of motion is then formulated in terms of the functional derivative

$$\frac{\delta \mathcal{L}_0}{\delta q^*} \equiv \frac{\partial \mathcal{L}_0}{\partial q^*} - \frac{d}{dt}\frac{\partial \mathcal{L}_0}{\partial q_t^*} - \frac{d}{dz}\frac{\partial \mathcal{L}_0}{\partial q_z^*} \tag{A9}$$

$$= i\varepsilon R[q,q^*]. \tag{A10}$$

Next we define

$$L_0 := \int_{-\infty}^{+\infty} dt\ \mathcal{L}_0. \tag{A11}$$

When we substitute the ansatz

$$q_0(z,t) = \eta(z)\ \mathrm{sech}[\nu(z)t] e^{(i\kappa(z)\log\{\mathrm{sech}(\nu(z)t)\} + i\sigma(z))}, \tag{A12}$$

with amplitude η, width ν, phase σ, and chirp κ, into the Lagrangian density $\mathcal{L}_0$ of the *unperturbed* NLSE, integration over time leads to the Lagrangian L_0 as a function of the parameters η, ν, κ, and σ and their space derivatives,

$$L_0 = \frac{\eta^2 \kappa \nu_z}{\nu^2} - \frac{2\eta^2 \sigma_z}{\nu} - \alpha_0 \frac{\eta^2 \kappa_z}{\nu} + \frac{2\eta^4}{3\nu} - \frac{1}{3}\eta^2 \nu(1+\kappa^2). \tag{A13}$$

Here, $\alpha_0 = -2 + 2\log 2$. When starting with some arbitrary initial conditions not agreeing with the parameters of an exact solution, the solutions (for $R \equiv 0$) of the Euler-Lagrange equations

$$\eta_z = \frac{\eta \kappa \nu^2}{3}, \tag{A14}$$

$$\nu_z = \frac{2\kappa \nu^3}{3}, \tag{A15}$$

$$\kappa_z = \frac{2}{3}(\eta^2 - \nu^2 - \kappa^2 \nu^2), \tag{A16}$$

$$\sigma_z = \frac{1}{6}[4\eta^2 - \nu^2 + \kappa^2 \nu^2 - 2\alpha_0(\eta^2 - \nu^2 + \kappa^2 \nu^2)] \tag{A17}$$

show oscillations of the parameters around the exact values.

To incorporate the influence of gain and damping, we follow the method presented in [32] for a perturbation $\varepsilon R[q,q^*] = \delta q + \beta q_{tt}$. The systematic perturbation theory leads to equations for the parameters $\Pi_i \in \{\eta, \nu, \kappa, \sigma\}$,

$$\begin{aligned}\frac{\delta L_0}{\delta \Pi_i} &\equiv \frac{\partial L_0}{\partial \Pi_i} - \frac{d}{dz}\frac{\partial L_0}{\partial \Pi_{i,z}} \\ &= \left[\frac{\partial}{\partial \Pi_i} - \frac{d}{dz}\frac{\partial}{\partial \Pi_{i,z}}\right] \\ &\quad \times \int_{-\infty}^{+\infty} dt\ \mathcal{L}_0(q,q^*,q_z,q_z^*,q_t,q_t^*) \\ &= \int_{-\infty}^{+\infty} dt \left[\frac{\delta \mathcal{L}_0}{\delta q}\frac{\partial q}{\partial \Pi_i} + \frac{\delta \mathcal{L}_0}{\delta q^*}\frac{\partial q^*}{\partial \Pi_i}\right] \\ &\approx \int_{-\infty}^{+\infty} dt \left[-i\varepsilon R^*[q_0,q_0^*]\frac{\partial q_0}{\partial \Pi_i} + i\varepsilon R[q_0,q_0^*]\frac{\partial q_0^*}{\partial \Pi_i}\right].\end{aligned} \tag{A18}$$

From here the modified Euler-Lagrange equations for $R \neq 0$ (i.e., $\delta \neq 0$ and $\beta \neq 0$) follow in the form

$$\eta_z = \delta\eta + \frac{\eta\ \kappa\ \nu^2}{3} - \frac{7}{9}\beta\ \eta\ \nu^2 - \frac{1}{9}\beta\ \eta\ \kappa^2\ \nu^2, \tag{A19}$$

$$\nu_z = \frac{2\ \kappa\ \nu^3}{3} - \frac{8}{9}\beta\ \nu^3 + \frac{4}{9}\beta\ \kappa^2\ \nu^3, \tag{A20}$$

$$\kappa_z = \frac{2}{3}(\eta^2 - \nu^2 - \beta\ \kappa\ \nu^2 - \kappa^2\ \nu^2 - \beta\ \kappa^3\ \nu^2). \tag{A21}$$

The fourth equation for the parameter σ decouples from the system (A19)–(A21) and yields (for constant η, ν, and κ) σ as a linear function of z,

$$\begin{aligned}\sigma_z = &\left(\frac{2}{3} - \frac{1}{3}\alpha_1\right)\eta^2 + \left(\frac{1}{3}\alpha_1 - \frac{1}{6}\right)\nu^2 + \left(\frac{2}{3}\alpha_1 + \frac{1}{2}\alpha_2 - \frac{1}{3}\alpha_3\right) \\ &\times \beta\kappa\nu^2 + \left(\frac{1}{6} + \frac{1}{3}\alpha_1\right)\kappa^2\nu^2 + \left(\frac{2}{3}\alpha_1 - \frac{2}{9}\alpha_4\right)\beta\kappa^3\nu^2.\end{aligned} \tag{A22}$$

We have introduced

$$\alpha_1 = \alpha_0 = -2 + 2\log 2, \quad \alpha_2 = -\frac{26}{9} + \frac{8}{3}\log 2, \tag{A23}$$

$$\alpha_3 = -5 + 6\log 2, \quad \alpha_4 = -4 + 3\log 2. \tag{A24}$$

It is noteworthy that the parameters of the exact solution (A2) are identical with the fixed point of the system (A19)–(A21).

Numerical simulations of the ODE model show an asymptotic approach of the initial pulse parameters to the stationary solution. Figure 6 displays a typical example for an initial pulse with $\eta > A$, $\nu > B$, and $\kappa > C$. Decaying oscillations in the pulse parameters occur; the final state corresponds to the exact solution (A2). The attraction by the solution (A2) is also shown in Fig. 7. The calculations agree with the simulations of Eq. (A1).

A stability analysis of the solution (A2) can be done within the ODE model, i.e., we investigate the stability of the parameters (A3) and (A4). Starting from perturbed parameters, a linearization of Eqs. (A19)–(A22) shows that the attractor is stable.

c. Perturbation theory

So far, we succeeded in modeling the correct behavior of the pulse by a (simple) momentum model. Still, in the math-

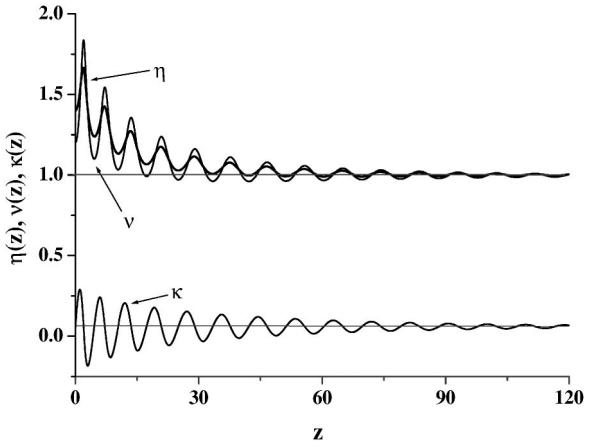

FIG. 6. Solution of the Euler-Lagrange equations (A19)–(A21) for $\delta=0.01$ and $\beta=0.03$.

ematically strict sense, the stability of the fixed point is not shown. To analyze the stability more exactly, a detailed investigation of Eq. (A1) itself is needed. Here, we perform the stability investigation by a multiple scales technique, searching for the first nonvanishing real part of the growth rate of a perturbation.

After separating the phase D, we split Eq. (A1) into the real and imaginary parts, i.e.,

$$q \equiv (a + ib)\exp[iDz], \tag{A25}$$

and obtain

$$a_z = -\frac{1}{2}b_{tt} - ba^2 - b^3 + Db + \epsilon\delta a + \epsilon\beta a_{tt}, \tag{A26}$$

$$b_z = \frac{1}{2}a_{tt} + ab^2 + a^3 - Da + \epsilon\delta b + \epsilon\beta b_{tt}. \tag{A27}$$

Here, we have indicated the smallness of δ and β by an additional factor ϵ to show the orders of perturbations and the different scales. (At the end we can set $\epsilon=1$.)

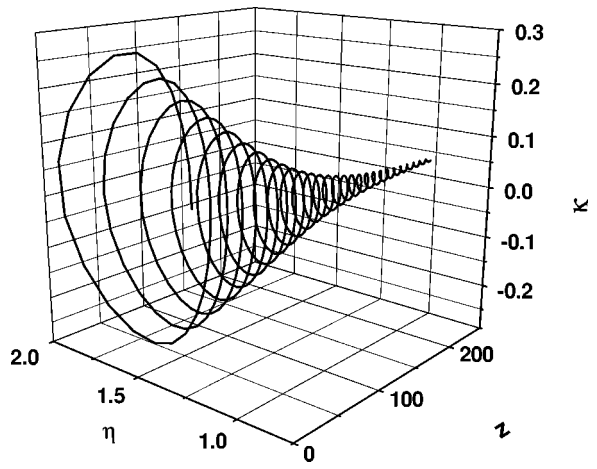

FIG. 7. Trajectory to the stable attractor in reduced parameter space for $\delta=0.01$ and $\beta=0.03$. Note that the attractor has a finite chirp κ.

While linearizing the equations at the fixed point $a=R$ and $b=J$, we assume the presence of small perturbations r and j,

$$a = R + r, \quad b = J + j, \tag{A28}$$

with a growth (damping) rate Γ, $r, j \sim \exp(\Gamma z)$. The expansions of R, J, as well as of r, j, and Γ are

$$R = R_0 + \epsilon R_1 + \epsilon^2 R_2 + \cdots, \tag{A29}$$

$$J = J_0 + \epsilon J_1 + \epsilon^2 J_2 + \cdots, \tag{A30}$$

$$r = r_0 + \epsilon^{1/2} r_{1/2} + \epsilon r_1 + \cdots, \tag{A31}$$

$$j = j_0 + \epsilon^{1/2} j_{1/2} + \epsilon j_1 + \cdots, \tag{A32}$$

$$\Gamma = \Gamma_0 + \epsilon^{1/2}\Gamma_{1/2} + \epsilon\Gamma_1 + \cdots. \tag{A33}$$

When we insert these expansions into Eqs. (A26) and (A27), we get relations (characterized by the orders in ϵ) which successively produce solvability conditions for $\Gamma_{i/2}$. Defining the operators

$$H_+ = -\frac{1}{2}\partial_{tt} - R_0{}^2 + \frac{3\delta}{2\beta}, \tag{A34}$$

$$H_- = \frac{1}{2}\partial_{tt} - 3R_0{}^2 + \frac{3\delta}{2\beta} \tag{A35}$$

leads to straightforward eigenvalue problems. Within the lowest order we get $\Gamma_0 r_0 = H_+ j_0$ and $\Gamma_0 j_0 = -H_- r_0$, yielding the solution $r_0=0, j_0=R_0$, and $\Gamma_0=0$. Calculating the order $\epsilon^{1/2}$, we obtain $0=H_+ j_{1/2}$ and $\Gamma_{1/2} j_0 = -H_- r_{1/2}$, with $j_{1/2}=j_0=R_0$ and $r_{1/2}=-H_-^{-1}\Gamma_{1/2} j_0$. We can derive an expression for $r_{i/2}$ in each step $i/2$. The further calculations show that $\Gamma_{1/2}$ also vanishes. Finally, Γ_1 is the essential rate, determining the stability of the pulse,

$$\Gamma \approx \epsilon\Gamma_1 = -\epsilon\frac{2}{3}\delta + i\epsilon\,\mathrm{Im}(\Gamma_1). \tag{A36}$$

Obviously, a stable situation exists as long as $\delta > 0$.

2. Modulational instability of the tails

A stability analysis of the ODE model shows that the attractor core is stable for $\delta > 0$. However, in order to get a stable stationary (long-living) solution in a broad time domain, balance between driving and damping is required in all regions. Imagine we have very long tails. Then, for $\delta > 0$, the tail becomes unstable to long-wavelength (slow) modulations. The reason is very simple. On the tail, perturbations proportional to $\exp(ikz - i\omega t)$ will be amplified by the term proportional to γq on the right-hand side of Eq. (A1) in the small-ω limit.

APPENDIX B: DETAILS OF THE GENERAL EULER-LAGRANGE EQUATIONS

Starting from the Lagrangian

$$L = \frac{2A^4}{3\eta} - \frac{1}{3}A^2\eta - \frac{1}{3}A^2C^2\eta - \frac{A^2\Omega^2}{\eta} - \frac{2A^2K'}{\eta} + \frac{2A^2\Omega T'}{\eta} + \frac{2A^2C'}{\eta} - \frac{\log[4]A^2C'}{\eta} + \frac{A^2C\eta'}{\eta^2}, \tag{B1}$$

the Euler-Lagrange equations are

$$\partial_z A = \frac{1}{9\eta}(A\{9\kappa_r A^2 - 9\sigma_i A^2\Omega + \eta^3[-7(\beta - 3\lambda_i\Omega) - C^2(\beta - 3\lambda_i\Omega) + 3C(1 + 6\lambda_r\Omega)] + \eta[A^2(8\chi - \sigma_r + \sigma_i C - 8\mu_i\Omega) + 9(\delta - \gamma\Omega - \beta\Omega^2 + \lambda_i\Omega^3)]\}), \tag{B2}$$

$$\partial_z \eta = \frac{1}{3A}(2\{-3\kappa_r A^3 + A^3[3\sigma_i\Omega + \eta(-2\chi + \sigma_r - \sigma_i C + 2\mu_i\Omega)] + A\eta[(1 + C^2)\eta^2(\beta - 3\lambda_i\Omega) + 3(-\delta + \gamma\Omega + \beta\Omega^2 - \lambda_i\Omega^3)] + 3\eta A'\}), \tag{B3}$$

$$\partial_z C = \frac{1}{3A\eta}(6\kappa_r A^3 C + 2A^3\{-3\sigma_i C\Omega + \eta[1 + \sigma_i(1 + 2C^2) + \mu_r\Omega + C(\chi - \sigma_r - \mu_i\Omega)]\} - 6C\eta A' + A\{-4C^3\eta^3(\beta - 3\lambda_i\Omega) - 2\eta^3(1 + 6\lambda_r\Omega) - 2C^2\eta^2(1 + 6\lambda_r\Omega) + C[-4\eta^3(\beta - 3\lambda_i\Omega) + 6\eta(\delta - \gamma\Omega - \beta\Omega^2 + \lambda_i\Omega^3) + 3\eta']\}), \tag{B4}$$

$$\partial_z T = -\mu_r A^2 - \frac{2}{3}\nu_r A^2 + \gamma C + \frac{1}{3}\mu_i A^2 C + \frac{\kappa_r A^2}{\eta^2} - \frac{\sigma_r A^2}{\eta} + \frac{\sigma_i A^2 C}{\eta} + \lambda_r\eta^2 - \frac{2}{3}\lambda_i C\eta^2 + \lambda_r C^2\eta^2 - \frac{2}{3}\lambda_i C^3\eta^2 + \Omega + 2\beta C\Omega - \frac{\sigma_i A^2\Omega}{\eta^2} + 3\lambda_r\Omega^2 - 3\lambda_i C\Omega^2, \tag{B5}$$

$$\partial_z\Omega = \frac{1}{15}\Bigg(10\kappa_i A^2 - 10\sigma_i A^2\eta - 10\sigma_i A^2C^2\eta - 10\gamma\eta^2 - 12\mu_i A^2\eta^2 - 8\nu_i A^2\eta^2 + 8\mu_r A^2C\eta^2 + 8\nu_r A^2C\eta^2 - 10\gamma C^2\eta^2 - 4\mu_i A^2C^2\eta^2 + 14\lambda_i\eta^4 + 20\lambda_i C^2\eta^4 + 6\lambda_i C^4\eta^4 - \frac{10\kappa_r A^2(C\eta - 3\Omega)}{\eta} + 30\delta\Omega + 20\chi A^2\Omega + 20\sigma_i A^2C\Omega - 30\beta\eta^2\Omega - 30\beta C^2\eta^2\Omega - 30\gamma\Omega^2 - 20\mu_i A^2\Omega^2 - \frac{30\sigma_i A^2\Omega^2}{\eta} + 60\lambda_i\eta^2\Omega^2 + 60\lambda_i C^2\eta^2\Omega^2 - 30\beta\Omega^3 + 30\lambda_i\Omega^4 - \frac{30\Omega A'}{A} + \frac{15\Omega\eta'}{\eta}\Bigg). \tag{B6}$$

[1] I. Aranson and L. Kramer, Rev. Mod. Phys. **74**, 99 (2002).
[2] A. Hasegawa and Y. Kodam, *Solitons in Optical Communications* (Oxford University Press, Oxford, 1955).
[3] N. Akhmediev and A. Ankiewicz, *Solitons Nonlinear Pulses and Beams* (Chapman & Hall, London, 1997).
[4] T. Brabec and F. Krausz, Phys. Rev. Lett. **78**, 3282 (1997).
[5] G. P. Agrawal, *Nonlinear Fiber Optics* (Academic, New York, 1995).
[6] Y. Kodama and A. Hasegawa, IEEE J. Quantum Electron. **23**, 510 (1987).
[7] L. Gagnon and P. A. Bélanger, Phys. Rev. A **43**, 6187 (1991).
[8] R. Hirota, J. Math. Phys. **14**, 805 (1973).
[9] N. Sasa and J. Satsuma, J. Phys. Soc. Jpn. **60**, 409 (1991).
[10] M. J. Potasek and M. Tabor, Phys. Lett. A **154**, 449 (1991).
[11] D. Mihalache, N. Truta, and L. C. Crasovan, Phys. Rev. E **56**, 1064 (1997).
[12] E. M. Gromov, L. V. Piskunova, and V. V. Tyutin, Phys. Lett. A **256**, 153 (1999).
[13] Z. H. Li, L. Li, H. P. Tian, and G. S. Zhou, Phys. Rev. Lett. **84**, 4096 (2000).
[14] V. I. Karpman, J. J. Rasmussen, and A. G. Shagalov, Phys. Rev. E **64**, 026614 (2001).
[15] S. L. Palacios, A. Guinea, J. M. Fernández-Díaz, and R. D. Crespo, Phys. Rev. E **60**, R45 (1999).
[16] M. Gedalin, T. C. Scott, and Y. B. Band, Phys. Rev. Lett. **78**, 448 (1997).
[17] V. I. Karpman, Phys. Rev. E **62**, 5678 (2000).
[18] A. Mahalingam and K. Porsezian, Phys. Rev. E **64**, 046608 (2001).
[19] K. J. Blow, N. J. Doran, and D. Wood, J. Opt. Soc. Am. B **6**, 1301 (1988).
[20] R. J. Deissler and H. R. Brand, Phys. Rev. Lett. **81**, 3856 (1998).
[21] N. Akhmediev, J. M. Soto-Crespo, and G. Town, Phys. Rev. E **63**, 056602 (2001).
[22] Z. H. Li, L. Li, H. P. Tian, G. S. Zhou, and K. H. Spatschek, Phys. Rev. Lett. **89**, 263901 (2002).
[23] H. R. Brand and R. J. Deissler, Phys. Rev. Lett. **63**, 2801 (1989).
[24] P. A. Bélanger, L. Gagnon, and C. Paré, Opt. Lett. **14**, 943 (1989).
[25] P. Kolodner, Phys. Rev. A **44**, 6466 (1991).
[26] G. K. Harkness, W. J. Firth, J. B. Geddes, J. V. Moloney, and E. M. Wright, Phys. Rev. A **50**, 4310 (1994).
[27] N. N. Akhmediev, M. J. Lederer, and B. Luther-Davies, Phys. Rev. E **57**, 3664 (1998).
[28] I. T. Sorokina, E. Sorokin, E. Wintner, A. Cassanho, H. P. Jenssen, and R. Szipocs, Opt. Lett. **22**, 1716 (1997).
[29] M. Nakazawa, K. Kurokawa, H. Kubota, and E. Yamada, Phys. Rev. Lett. **65**, 1881 (1990).
[30] K. Kurokawa and M. Nakazawa, Appl. Phys. Lett. **58**, 2871 (1991).
[31] N. R. Pereira and L. Stenflo, Phys. Fluids **20**, 1733 (1977).
[32] A. Hasegawa, Pramana, J. Phys. **57**, 1097 (2001).